

## Electronic Supplementary Information

### Stabilizing black-phase FAPbI<sub>3</sub> in humid air with secondary ammoniums

Ruixue Lu,<sup>ab</sup> Yang Liu,<sup>b</sup> Dongyuan Zhao,<sup>a</sup> Xin Guo<sup>\*b</sup> and Can Li<sup>\*bc</sup>

<sup>a</sup> *Department of Chemistry, iChEM (Collaborative Innovation Center of Chemistry for Energy Materials), Fudan University, 2205 Songhu Road, Shanghai 200438, PR China*

<sup>b</sup> *State Key Laboratory of Catalysis, Dalian Institute of Chemical Physics, Chinese Academy of Sciences, Dalian National Laboratory for Clean Energy, 457 Zhongshan Road, Dalian 116023, China*

<sup>c</sup> *University of Chinese Academy of Sciences, Beijing, 100049, PR China*

\* E-mail: [guoxin@dicp.ac.cn](mailto:guoxin@dicp.ac.cn); [canli@dicp.ac.cn](mailto:canli@dicp.ac.cn)

## **Experimental Procedures**

### **Solar cell fabrications**

The electron transport layer prepared by spin-coating SnO<sub>2</sub> nanoparticle (3%, diluted by water) at 4000 r.p.m. for 30 s on cleaned ITO and annealed in ambient air at 150 °C for 30 mins. After cooled down to room temperature, the substrates were cleaned with ultraviolet ozone for 20 mins to improve the surface wetting before next step. Perovskite active layers were fabricated by two-step interdiffusion process, where 1.4 M of PbI<sub>2</sub> in DMF/DMSO (v/v 94/6) solvent was spin-coated onto SnO<sub>2</sub> layer and annealed at 70 °C for 1 min, after the film cooled down to room temperature, a solution of 70 mg FAI and 10 mg MACl in 1 mL iPA with/without 1.5 × 10<sup>-5</sup> mmol (2.6, 3.0 and 3.4 mg/mL for DMA, DEA and DiPA respectively) secondary ammonium was spin-coated on the PbI<sub>2</sub>, then the films were annealed at 150 °C for 15 mins in ambient air conditions (30% ~ 40% relative humidity (RH)). After the perovskite films cooled to room temperature, spiro-OMeTAD solution (prepared by dissolving 72.3 mg spiro-OMeTAD in 1 mL chlorobenzene, to which 28.8 μL 4-tert-butyl pyridine and 17.5 μL lithium bis(trifluoromethanesulfonyl)imide solution of 520 mg LITFSI in 1 mL acetonitrile were added) was deposited on the perovskite films at 3500 rpm for 30 s. Finally, 100 nm gold electrode was thermally evaporated under vacuum of ~ 10<sup>-6</sup> Torr, at a rate of ~ 0.2 Å/s and the active area is 0.04 cm<sup>2</sup>.

### **Characterization methods**

The J-V measurement was performed via the solar simulator (SS-F5-3A, Enlitech) along with AM 1.5G spectra whose intensity was calibrated by the certified standard silicon solar cell (SRC-2020, Enlitech) at 100 mW cm<sup>-2</sup>. The external quantum efficiency (EQE) data were obtained by using the solar-cell spectral-response measurement system (QE-R, Enlitech). Light intensity-dependent J-V curves were obtained by tuning the light source powder and calibrating it with the current of the silicon solar cell with a KG5 filter.

X-ray diffraction (XRD) analysis was conducted with a Bruker D2 Phaser diffractometer using Cu Kα radiation provided applied current and voltage values of

200 mA and 40 kV, respectively. The diffraction data were collected with angular range 5–50° (2 theta) with step size 0.02. UV-Vis absorption spectra were measured by Cary 5000 UV-Vis NIR spectrophotometer, Varian Inc, USA. The morphology of the perovskite films was investigated by scanning electron microscopy (SEM) on a Quanta 200F microscope (FEI Company) with an accelerating voltage of 20 kV. Grazing-incidence wide-angle X-ray diffraction (GIXRD) data were obtained using the Beamline BL14B1 of the Shanghai Synchrotron Radiation Facility (SSRF) with the incident photon energy of 10 keV (wavelength of 1.2398 Å) at an incident angle of 0.4° and an exposure time of 30 s. The steady-state PL spectra and time-resolved PL spectra were recorded on a FLS920 fluorescence spectrometer (Edinburgh Instruments) in air at room temperature. A picosecond pulsed diode laser (406.8 nm) was used as the excitation source. X-ray photoelectron spectroscopy (XPS) was carried out on an ESCALAB 250Xi photoelectron spectroscopy (Thermo Fisher Scientific) with Al K $\alpha$  radiation source and all the binding energies were calibrated by C 1s (284.8 eV) as a reference. Electrochemical impedance spectroscopy (EIS) measurements were performed with a bias of 0.9 V in the frequency range of 1 MHz to 1 Hz in dark condition at room temperature using an electrochemical workstation (CHI600D).

### **SCLC**

The relationship between the trap filled limit voltage ( $V_{TFL}$ ), applied voltage at the first kink point, and trap state density ( $N_t$ , also known as tDOS) is shown in Equation (S1):

$$V_{TFL} = \frac{eN_t d^2}{2\epsilon_0 \epsilon} \quad (S1)$$

Where  $d$  is thickness of perovskite film,  $\epsilon$  is the relative dielectric constant (for FAPbI<sub>3</sub>,  $\epsilon \approx 49.4$ ), and  $\epsilon_0$  ( $8.85 \times 10^{-12}$ ) is the constant of permittivity in free space.

### **TRPL**

TRPL was conducted to analyze carrier lifetime and extraction. Carrier lifetimes can be extracted from TRPL quenching feature of perovskite films as illustrated by Equation (S2):

$$f(t) = A + B_1 \exp\left(-\frac{t}{\tau_1}\right) + B_2 \exp\left(-\frac{t}{\tau_2}\right) \quad (\text{S2})$$

where  $A$  is a constant for the baseline offset,  $B_1$  and  $B_2$  are the relative amplitudes,  $\tau_1$  and  $\tau_2$  are the carrier lifetimes for the fast and slow recombination, respectively.

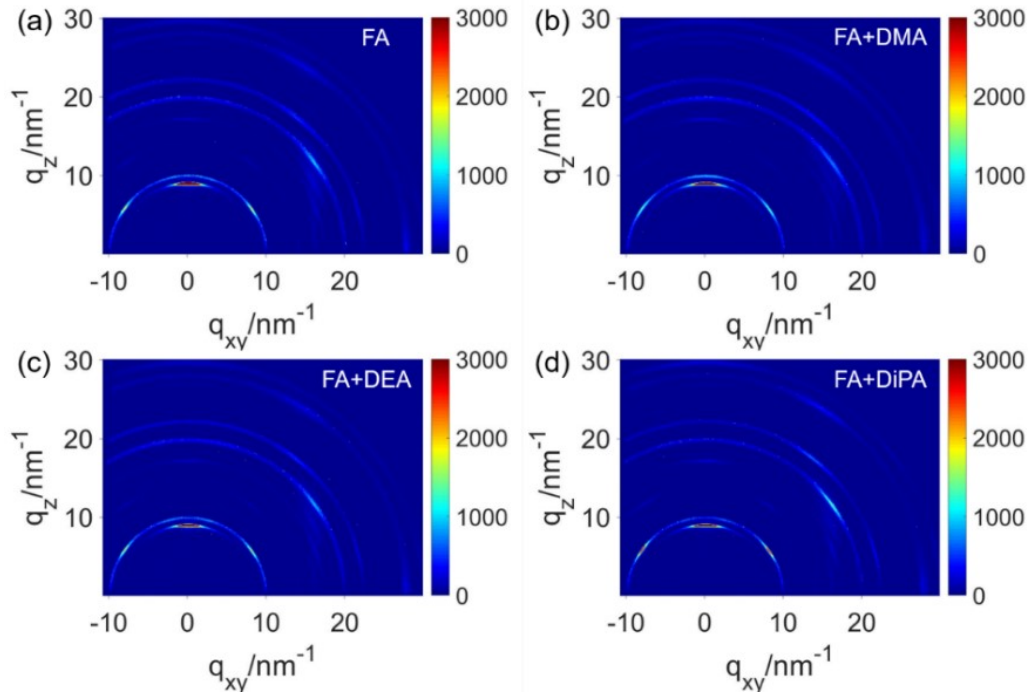


**Fig. S1.** 2D GIXRD data of the (a) FA, (b) FA+DMA, (c) FA+DEA and (d) FA+DiPA films.

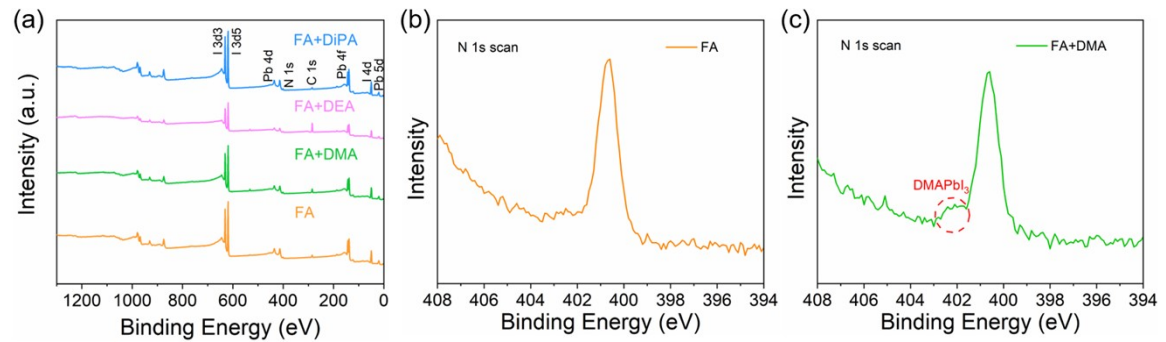


**Fig. S2.** (a) XPS survey spectra of the FAPbI<sub>3</sub> films with and without additives. XPS of N 1s core-level spectra for the (b) FA and (c) FA+DMA films.

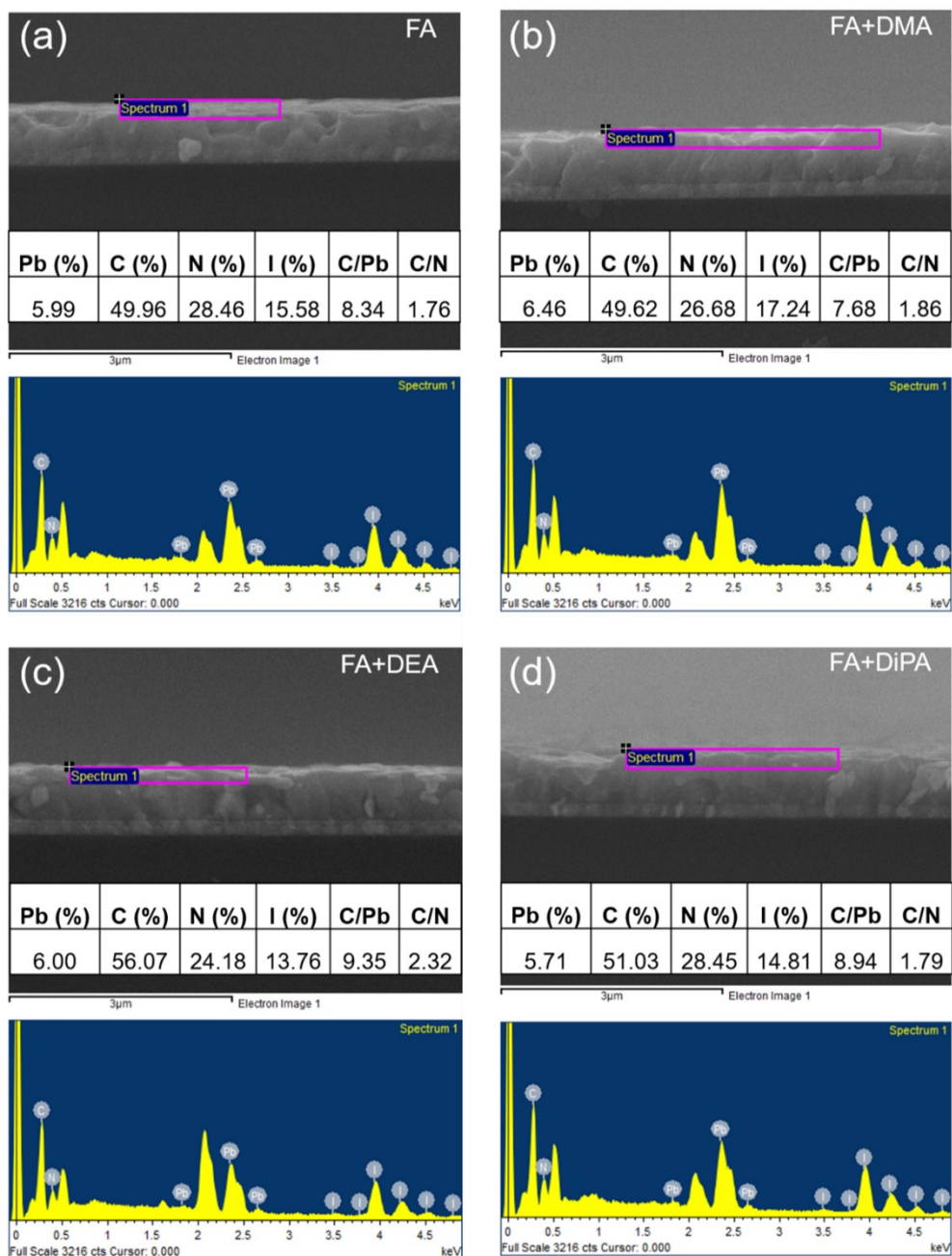


**Fig. S3.** Surface EDS of the (a) FA, (b) FA+DMA, (c) FA+DEA and (d) FA+DiPA films.

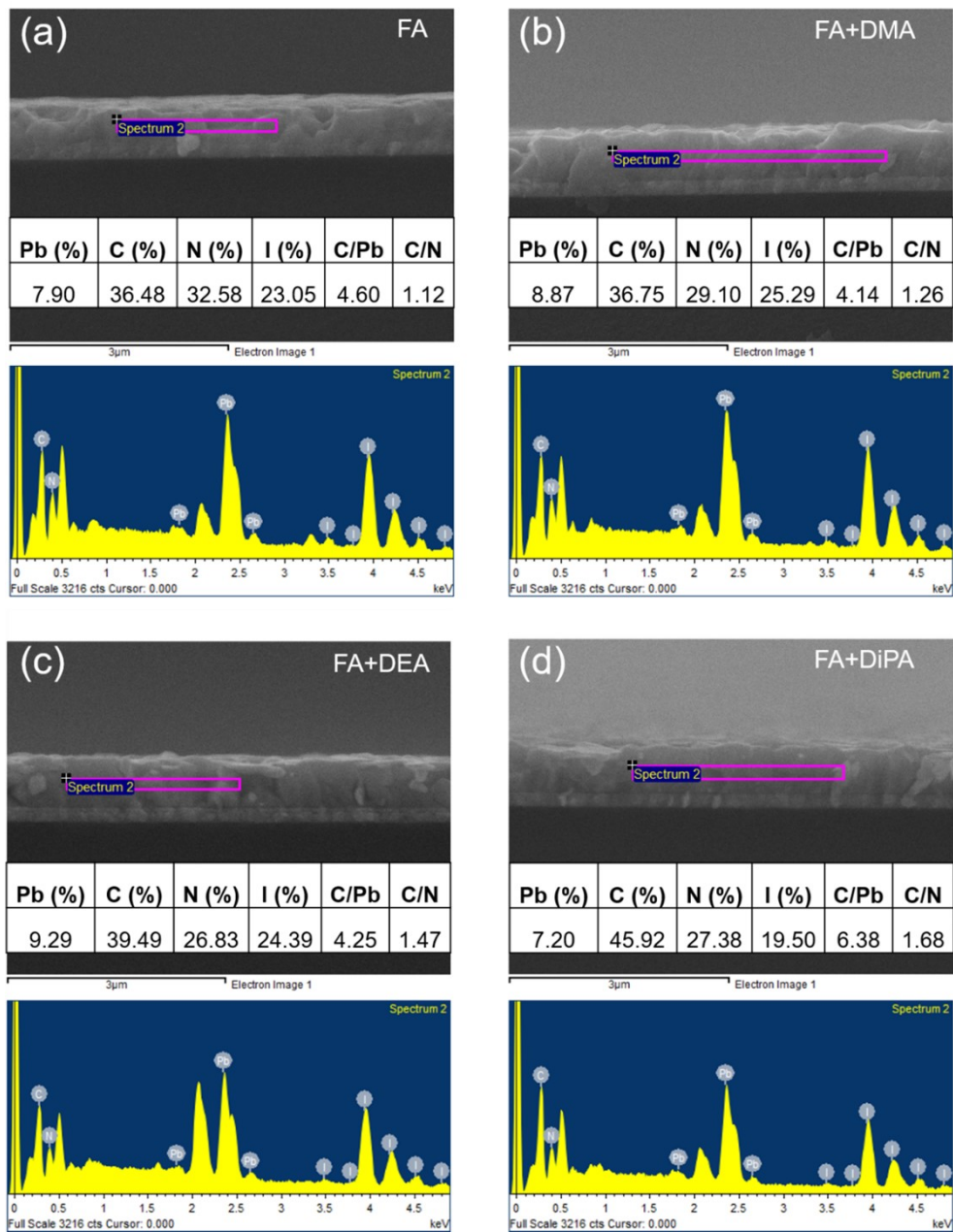


**Fig. S4.** Bulk EDS of the (a) FA, (b) FA+DMA, (c) FA+DEA and (d) FA+DiPA films.

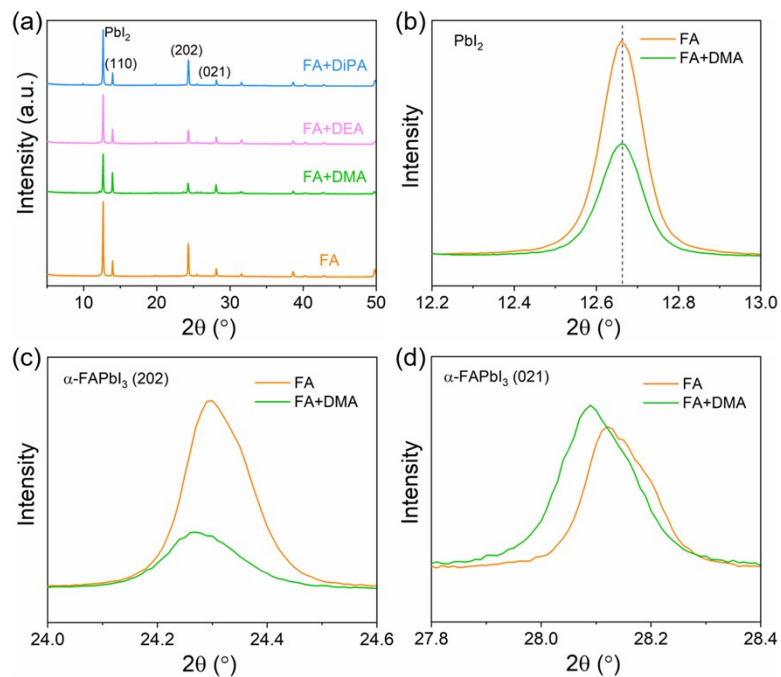


**Fig. S5.** (a) XRD patterns of the FAPbI<sub>3</sub> films with and without additives. (b-d) Magnified XRD patterns of the FA and FA+DMA samples.

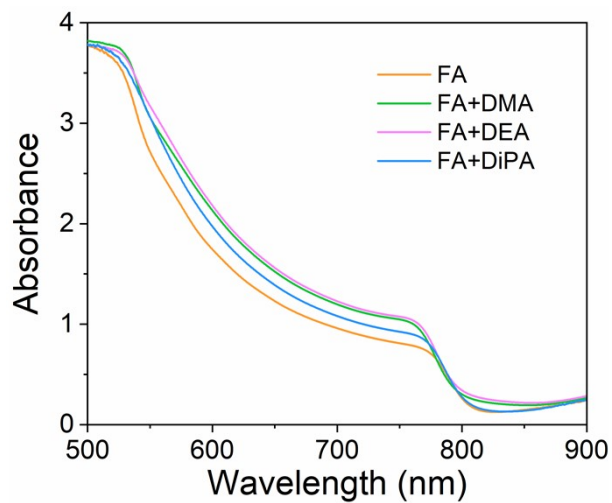


**Fig. S6.** UV-Vis absorption spectra of perovskite films with and without additives.

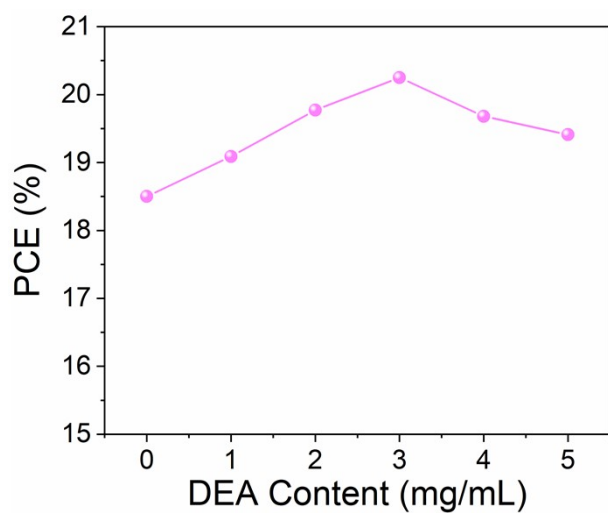


**Fig. S7.** PCE evolution with DEA content.

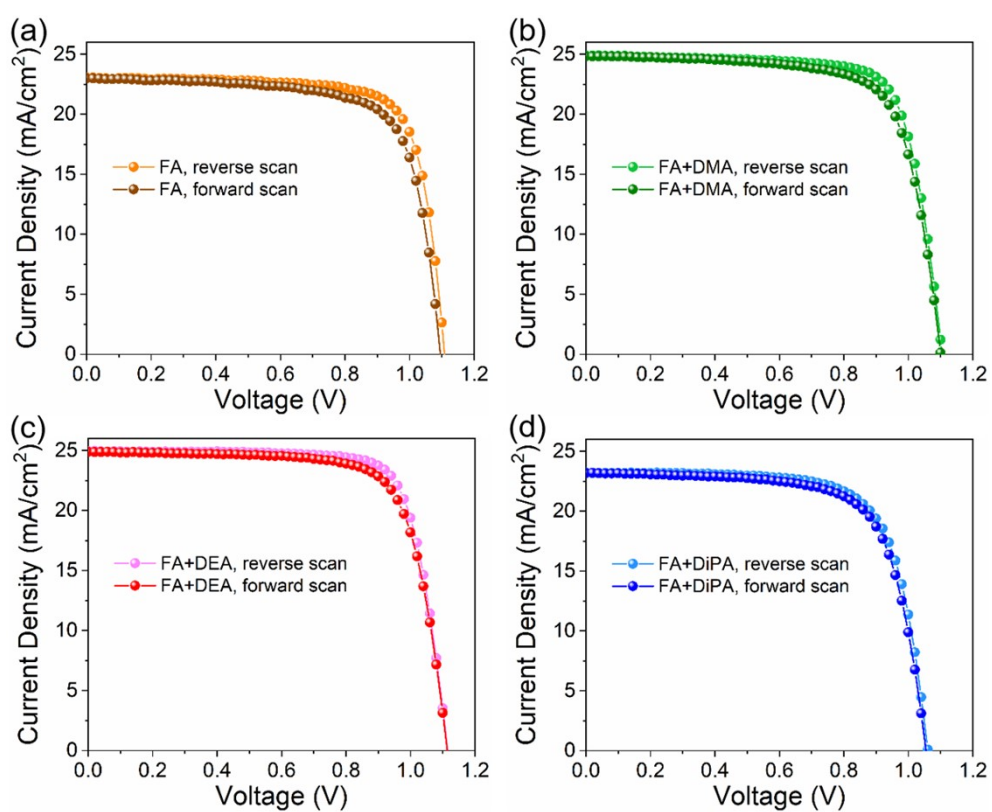


**Fig. S8.** Hysteresis of PSCs based on the (a) FA, (b) FA+DMA, (c) FA+DEA and (d) FA+DiPA films.



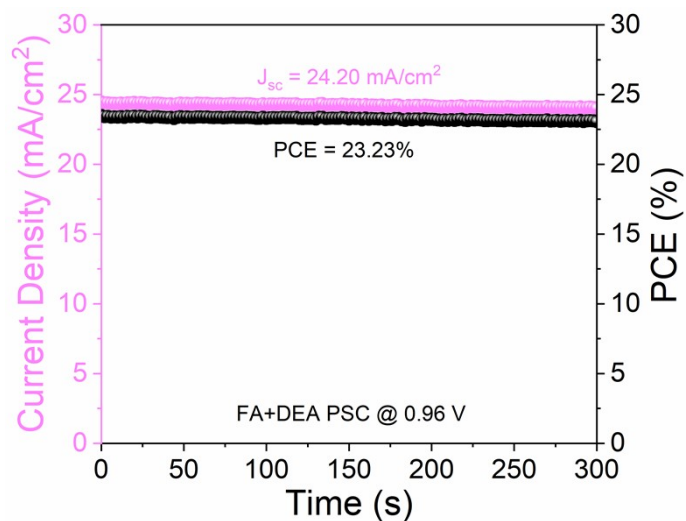


**Fig. S9.** Steady-state photocurrent and efficiency measured at the maximum power point (0.96 V) of the FA+DEA PSC.

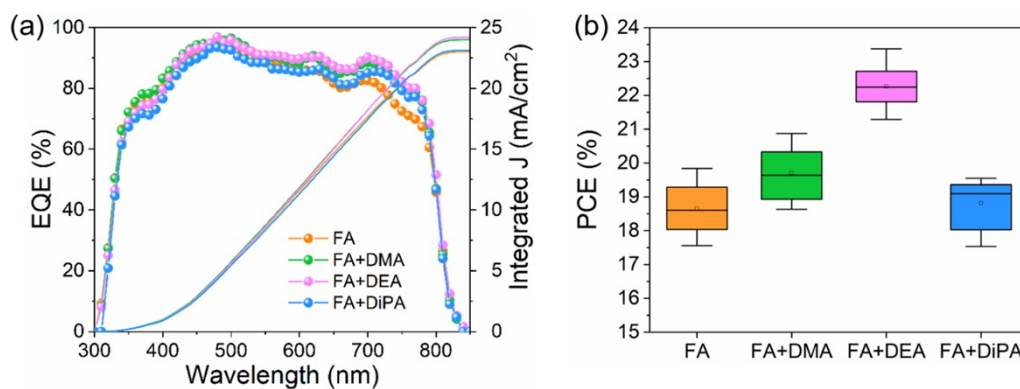


**Fig. S10.** (a) EQE curves and (b) PCE distribution (15 devices) of the FAPbI<sub>3</sub> PSCs with and without additives.

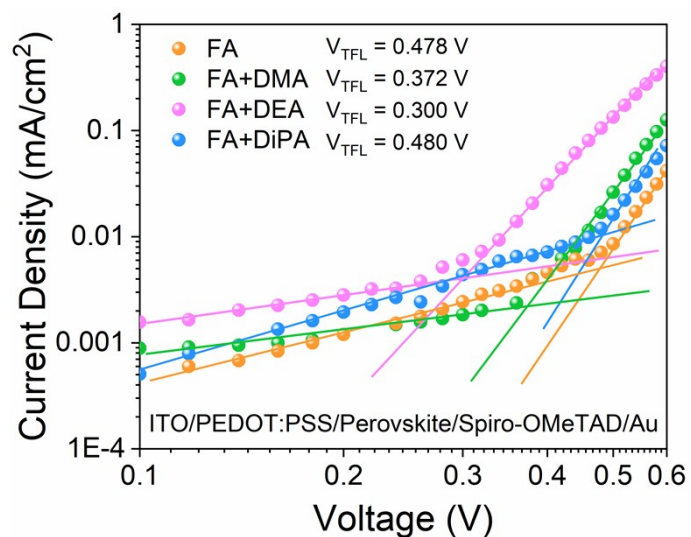


**Fig. S11.** J-V characteristics of hole-only devices with ITO/PEDOT:PSS/perovskite/Spiro-OMeTAD/Au configuration.

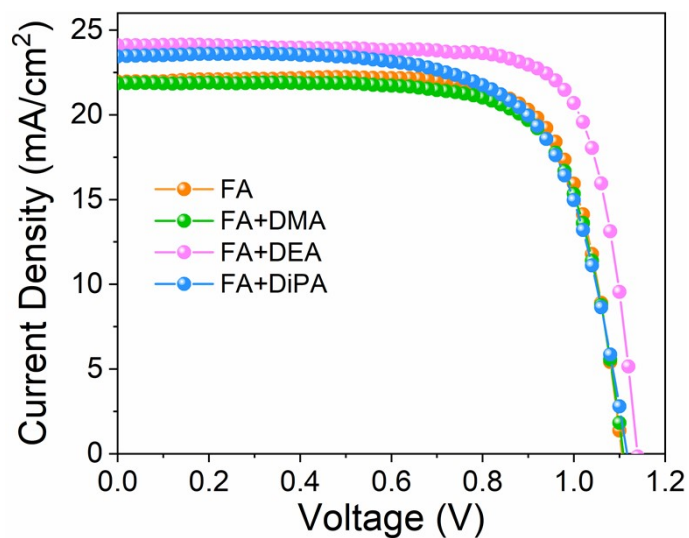


**Fig. S12.** J-V curves of the PSCs with PBDB-T as HTL.

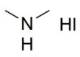
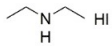
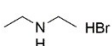
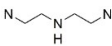
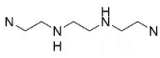
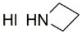
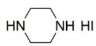
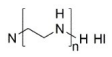
**Table S1.** Humidity stability of primary ammonium-treated FAPbI<sub>3</sub> perovskite films and/or PSCs in literature.<sup>[a]</sup>

Year	Primary ammonium	Structure	Humidity stability performance	PCE	Reference
2016	PEAI	p-i-n	<50% RH	17.7%	1
2016	Benzylamine	n-i-p	PCE>50% (50%±5% RH, 4 months) No $\delta$ -FAPbI <sub>3</sub> (70±5% RH, 80 days)	19.2%	2
2017	MACl	p-i-n	/	20.6%	3
2019	PEAI	n-i-p	/	23.56% (23.32%) <sup>[b]</sup>	4
2019	MACl	n-i-p	/	24.02% (23.48%) <sup>[b]</sup>	5
2019	methylenediammonium dichloride	n-i-p	PCE>90% (85% RH, 70h; HTL: copper phthalocyanine)	24.66% (23.73%) <sup>[b]</sup>	6
2020	p-phenyl dimethylammonium iodide	n-i-p	No $\delta$ -FAPbI <sub>3</sub> (70% RH, 4h)	21.47%	7
2020	MASCN/FASCN	n-i-p	/	23.1%	8
2020	phenylmethylammonium iodide	n-i-p	<50% RH	23.32%	9
2020	methylenediammonium dichloride Csl	n-i-p	/	25.17% (24.37%) <sup>[b]</sup>	10
2021	n-propylammonium chloride	n-i-p	PCE>70% for 700h under 60%RH (PCE<80% for 100h)	22.22%	11
2021	methylamine formate	n-i-p	/	24.1%	12
2021	4-tert-butyl-benzylammonium iodide FACl	n-i-p	<50% RH	20.92%	13

<sup>[a]</sup> All the works listed contain no low-dimensional perovskite and Br components.

<sup>[b]</sup> Certified efficiency.

**Table S2.** Summary of secondary ammoniums applied in PSCs in literature.

Secondary ammonium	Perovskite	Structure	PCE	Reference
	$\text{Cs}_{0.7}\text{DMA}_{0.3}\text{PbI}_3$	p-i-n	12.62%	14
	$\text{CsPbI}_3$	n-i-p	19.03%	15
DMAI	$\text{MA}_{1-x}\text{DMA}_x\text{PbI}_3$	p-i-n	21.6%	16
	$\text{FA}_x\text{Cs}_{1-x}\text{PbI}_y\text{Br}_{3-y}$	p-i-n	<18%	17
	$\text{Cs}_{0.05}\text{FA}_{0.85}\text{MA}_{0.10}\text{Pb}(\text{I}_{0.97}\text{Br}_{0.03})_3$	n-i-p	22.61%	18
	$(\text{DA}_2\text{PbI}_4)_{0.05}\text{MAPbI}_3$	n-i-p	19.05%	19
DEAI				
DEAI				
	$(\text{DA}_2\text{PbI}_2\text{Br}_2)_{0.05}\text{MAPbI}_3$	n-i-p	19.58%	20
DEABr				
	$\text{MAPbI}_3$	p-i-n	20.13%	21
Diethylenetriamine				
	$\text{Cs}_{0.05}\text{MA}_{0.16}\text{FA}_{0.79}\text{PbI}_{2.5}\text{Br}_{0.5}$	n-i-p	18.09%	22
Diethylenetriamine and triethylenetetramine			18.03%	
	$\text{Cs}_{0.05}(\text{FA}_{0.9}\text{MA}_{0.1})_{0.95}\text{Pb}(\text{I}_{0.9}\text{Br}_{0.1})_3$	n-i-p	22.39	23
Azetidinium iodide				
	$\text{Cs}_{0.05}(\text{FA}_{0.95}\text{MA}_{0.05})_{0.95}\text{Pb}(\text{I}_{0.95}\text{Br}_{0.05})_3$	p-i-n	23.37%	24
Piperazininium iodide			(22.75%) <sup>[a]</sup>	
	$\text{MAPbI}_3$	p-i-n	19.23%	25
Polyethylenimine iodide				

<sup>[a]</sup> Certified efficiency.

**Table S3.** Percentage composition of different perovskite films according to XPS.

Sample	Pb (%)	C (%)	N (%)	I (%)	Cl (%)	C/Pb
FA	15.51	35.53	9.93	35.78	3.25	2.29
FA+DMA	11.06	50.96	9.38	25.47	3.12	4.61
FA+DEA	4.38	76.90	6.07	10.70	1.94	17.56
FA+DiPA	16.32	28.48	11.93	40.16	3.11	1.75

**Table S4.** Detailed fitting parameters of perovskite films from TRPL measurement.

Sample	$\tau_1$ [ns]	$B_1$	$\tau_2$ [ns]	$B_2$	$\tau_{ave}$ [ns]
FA	123.56	954.05	1072.96	1750.65	1016.85
FA+DMA	127.33	1044.39	1437.87	1704.64	1370.38
FA+DEA	150.87	726.06	1622.29	2039.75	1575.20
FA+DiPA	122.58	912.28	915.06	1806.40	864.82

**Table S5.** Detailed fitting parameters of perovskite films with charge transport layers from TRPL measurement.

Sample	$\tau_1$ [ns]	$B_1$	$\tau_2$ [ns]	$B_2$	$\tau_{ave}$ [ns]
FA/ETL	46.16	596.25	190.51	1245.86	175.51
FA+DMA/ETL	40.20	825.23	182.83	1051.57	161.84
FA+DEA/ETL	44.01	862.67	172.33	923.70	147.62
FA+DiPA/ETL	44.27	739.36	170.53	1127.22	152.16
FA/HTL	32.71	1558.63	261.38	136.86	127.00
FA+DMA/HTL	20.28	1274.03	261.41	312.51	203.47
FA+DEA/HTL	18.64	1631.42	248.65	81.22	110.46
FA+DiPA/HTL	40.02	1469.37	226.99	155.53	110.17

**Table S6.** Photovoltaic parameters of PSCs without additive.

Device	$V_{oc}$ [V]	$J_{sc}$ [mA/cm <sup>2</sup> ]	FF [%]	PCE [%]
1	1.11	23.13	77.11	19.84
2	1.11	23.28	75.68	19.59
3	1.06	23.99	76.66	19.50
4	1.08	23.40	76.12	19.29
5	1.08	22.67	78.32	19.25
6	1.08	23.40	75.31	19.03
7	1.07	23.53	74.00	18.68
8	1.08	23.27	73.76	18.60
9	1.09	23.02	72.62	18.31
10	1.07	22.33	76.41	18.25
11	1.06	23.29	73.67	18.13
12	1.06	23.41	72.36	18.04
13	1.07	22.30	74.87	17.81
14	1.09	22.52	71.48	17.56
15	1.07	23.80	70.75	17.94

**Table S7.** Photovoltaic parameters of PSCs with DMA additive.

Device	$V_{oc}$ [V]	$J_{sc}$ [mA/cm <sup>2</sup> ]	FF [%]	PCE [%]
1	1.11	24.90	75.86	20.87
2	1.10	25.17	73.98	20.54
3	1.08	24.37	76.72	20.13
4	1.09	24.54	75.97	20.41
5	1.11	22.97	79.46	20.33
6	1.10	24.85	73.73	20.16
7	1.14	24.81	69.92	19.73
8	1.10	23.51	75.90	19.64
9	1.06	24.35	75.68	19.53
10	1.08	23.13	78.07	19.50
11	1.06	23.05	75.93	18.63
12	1.08	24.35	74.03	19.39
13	1.08	22.29	78.64	18.88
14	1.08	22.82	76.97	18.88
15	1.10	23.14	74.32	18.93

**Table S8.** Photovoltaic parameters of PSCs with DEA additive.

Device	$V_{oc}$ [V]	$J_{sc}$ [mA/cm <sup>2</sup> ]	FF [%]	PCE [%]
1	1.18	25.17	78.99	23.38
2	1.17	24.93	79.02	23.03
3	1.18	25.00	77.93	22.89
4	1.14	25.55	76.65	22.25
5	1.17	24.82	77.74	22.65
6	1.14	25.20	77.77	22.41
7	1.17	24.76	77.04	22.35
8	1.13	25.50	77.31	22.24
9	1.14	25.20	77.77	22.41
10	1.14	24.96	77.36	22.09
11	1.17	23.84	78.73	21.95
12	1.14	25.63	74.08	21.72
13	1.12	25.14	76.62	21.63
14	1.13	24.83	76.52	21.43
15	1.14	23.95	78.13	21.28

**Table S9.** Photovoltaic parameters of PSCs with DiPA additive.

Device	$V_{oc}$ [V]	$J_{sc}$ [mA/cm <sup>2</sup> ]	FF [%]	PCE [%]
1	1.07	23.85	75.86	19.36
2	1.05	23.60	71.58	17.78
3	1.07	23.53	69.58	17.54
4	1.07	23.95	75.49	19.41
5	1.08	23.92	74.68	19.29
6	1.06	23.70	73.41	18.51
7	1.07	23.72	70.39	17.85
8	1.07	23.98	74.43	19.18
9	1.07	23.96	75.74	19.45
10	1.07	23.76	74.62	19.01
11	1.08	23.75	73.60	18.89
12	1.07	23.55	71.31	18.03
13	1.08	23.91	75.90	19.55
14	1.07	23.76	75.21	19.09
15	1.08	23.72	75.30	19.29

## References

1. N. Li, Z. Zhu, C.-C. Chueh, H. Liu, B. Peng, A. Petrone, X. Li, L. Wang and A. K. Y. Jen, *Adv. Energy Mater.*, 2017, **7**, 1601307.
2. F. Wang, W. Geng, Y. Zhou, H. H. Fang, C. J. Tong, M. A. Loi, L. M. Liu and N. Zhao, *Adv. Mater.*, 2016, **28**, 9986-9992.
3. F. Xie, C.-C. Chen, Y. Wu, X. Li, M. Cai, X. Liu, X. Yang and L. Han, *Energy Environ. Sci.*, 2017, **10**, 1942-1949.
4. Q. Jiang, Y. Zhao, X. Zhang, X. Yang, Y. Chen, Z. Chu, Q. Ye, X. Li, Z. Yin and J. You, *Nat. Photon.*, 2019, **13**, 460-466.
5. M. Kim, G.-H. Kim, T. K. Lee, I. W. Choi, H. W. Choi, Y. Jo, Y. J. Yoon, J. W. Kim, J. Lee, D. Huh, H. Lee, S. K. Kwak, J. Y. Kim and D. S. Kim, *Joule*, 2019, **3**, 2179-2192.
6. H. Min, M. Kim, S.-U. Lee, H. Kim, G. Kim, K. Choi, J. H. Lee and S. I. Seok, *Science*, 2019, **366**, 749-753.
7. M. Hou, Y. Xu, B. Zhou, Y. Tian, Y. Wu, D. Zhang, G. Wang, B. Li, H. Ren, Y. Li, Q. Huang, Y. Ding, Y. Zhao, X. Zhang and G. Hou, *Adv. Funct. Mater.*, 2020, **30**, 2002366.
8. H. Lu, Y. Liu, P. Ahlawat, A. Mishra, W. R. Tress, F. T. Eickemeyer, Y. Yang, F., Z. Wang, C. E. Avalos, B. I. Carlsen, A. Agarwalla, X. Zhang, X. Li, Y. Zhan, S. M. Zakeeruddin, L. Emsley, U. Rothlisberger, L. Zheng, A. Hagfeldt and M. Grätzel, *Science*, 2020, **370**, eabb8985.
9. X. Yang, Y. Fu, R. Su, Y. Zheng, Y. Zhang, W. Yang, M. Yu, P. Chen, Y. Wang, J. Wu, D. Luo, Y. Tu, L. Zhao, Q. Gong and R. Zhu, *Adv. Mater.*, 2020, **32**, 2002585.
10. G. Kim, H. Min, K. S. Lee, D. Y. Lee, S. M. Yoon and S. I. Seok, *Science*, 2020, **370**, 108-112.
11. Y. Zhang, Y. Li, L. Zhang, H. Hu, Z. Tang, B. Xu, and N.-G. Park, *Adv. Energy Mater.*, 2021, **11**, 2102538.
12. W. Hui, L. Chao, H. Lu, F. Xia, Q. Wei, Z. Su, T. Niu, L. Tao, B. Du, D. Li, Y. Wang, H. Dong, S. Zuo, B. Li, W. Shi, X. Ran, P. Li, H. Zhang, Z. Wu, C. Ran, L. Song, G. Xing, X. Gao, J. Zhang, Y. Xia, Y. Chen and W. Huang, *Science*, 2021, **371**, 1359-1364.
13. X. Ling, H. Zhu, W. Xu, C. Liu, L. Pan, D. Ren, J. Yuan, B. W. Larson, C. Gratzel, A. R. Kirmani, O. Ouellette, A. Krishna, J. Sun, C. Zhang, Y. Li, S. M. Zakeeruddin, J. Gao, Y. Liu, J. R. Durrant, J. M. Luther, W. Ma and M. Grätzel, *Angew. Chem., Int. Ed.*, 2021, **60**, 27299-27306.
14. W. Ke, I. Spanopoulos, C. C. Stoumpos and M. G. Kanatzidis, *Nat. Commun.*, 2018, **9**, 4785.
15. Y. Wang, X. Liu, T. Zhang, X. Wang, M. Kan, J. Shi and Y. Zhao, *Angew. Chem., Int. Ed.*, 2019, **58**, 16691-16696.
16. H. Chen, Q. Wei, M. I. Saidaminov, F. Wang, A. Johnston, Y. Hou, Z. Peng, K. Xu, W. Zhou, Z. Liu, L. Qiao, X. Wang, S. Xu, J. Li, R. Long, Y. Ke, E. H. Sargent and Z. Ning, *Adv. Mater.*, 2019, **31**, 1903559.
17. G. E. Eperon, K. H. Stone, L. E. Mundt, T. H. Schloemer, S. N. Habisreutinger, S. P. Dunfield, L. T. Schelhas, J. J. Berry and D. T. Moore, *ACS Energy Lett.*, 2020, **5**, 1856-1864.
18. J. Sun, X. Zhang, X. Ling, Y. Yang, Y. Wang, J. Guo, S. Liu, J. Yuan and W. Ma, *J. Mater. Chem. A.*, 2021, **9**, 23019-23027.
19. X. Huang, Q. Cui, W. Bi, L. Li, P. Jia, Y. Hou, Y. Hu, Z. Lou and F. Teng, *RSC Adv.*, 2019, **9**, 7984-7991.
20. X. Huang, W. Bi, P. Jia, Q. Cui, Y. Hu, Z. Lou, Y. Hou and F. Teng, *ACS Appl. Mater. Interfaces*, 2020, **12**, 16707-16714.



21. H. Zhang, X. Ren, X. Chen, J. Mao, J. Cheng, Y. Zhao, Y. Liu, J. Milic, W.-J. Yin, M. Grätzel and W. C. H. Choy, *Energy Environ. Sci.*, 2018, **11**, 2253-2262.
22. D. Yao, X. Mao, X. Wang, Y. Yang, M. T. Hoang, A. Du, E. R. Waclawik, G. J. Wilson and H. Wang, *J. Power Sources*, 2020, **463**, 228210.
23. F. Ansari, E. Shirzadi, M. Salavati-Niasari, T. LaGrange, K. Nonomura, J. H. Yum, K. Sivula, S. M. Zakeeruddin, M. K. Nazeeruddin, M. Grätzel, P. J. Dyson and A. Hagfeldt, *J. Am. Chem. Soc.*, 2020, **142**, 11428-11433.
24. F. Li, X. Deng, F. Qi, Z. Li, D. Liu, D. Shen, M. Qin, S. Wu, F. Lin, S. H. Jang, J. Zhang, X. Lu, D. Lei, C. S. Lee, Z. Zhu and A. K. Jen, *J. Am. Chem. Soc.*, 2020, **142**, 20134-20142.
25. C. Wang, H. Yang, X. Xia, X. Wang and F. Li, *Appl. Surf. Sci.*, 2021, **548**, 149276.